Simulating Pathological Gait using the Enhanced Inverted Pendulum Model

Taku Komura, Akinori Nagano, Shunsuke Kudoh, Yoshihisa Shinagawa

February 5, 2004

Abstract

In this study, we propose a new method to simulate human gait motion when the muscles are deactivated. The method is based on the inverted pendulum model that is used for gait generation in robotics. After the normal gait motion is generated by setting the initial posture and the value of the parameters that determine the motion, the muscle to be deactivated is specified. By minimizing an objective function based on the force exerted by the specified muscle during the motion, the set of parameters that represent the pathological gait is calculated. The effects of weakening the gluteus medialis muscles was analyzed. The data of the final motion was compared with data by real patients and there were significant similarities among them. Since the number of parameters to describe the motion is limited in our method, the optimization process converges much faster than previous methods.

1 Introduction

Techniques to simulate human gait motion have been developed by researchers in areas such as biomechnaics and robotics. The mehtods used in each area is based on different methods.

In biomechanics, computer simulations based on musculoskeletal models are often used to analyze the role of specific muscles during motions. Many researchers have analyzed the contribution of some specific muscles to performance by using optimization methods based on forward dynamics [19]. For example, Pandy et al.[20] analyzed the role of biarticular muscles in maximal jumping, and they concluded that biarticular muscles contribute to jumping performance by redistributing segmental energy within the musculoskeletal system but without generating energy by themselves (a conclusion that is consistent with that made by Rocobs et al. [8]). Neptune et al. [18] analyzed the role of the plantarflexor muscles during gait, and they calculated the degree to which these muscles contribute to propelling the trunk in the forward direction (induced acceleration [24]). Piazza et al.[22] examined the contribution of muscle forces to knee flexion during the swing phase of normal gait. However, the effects of muscle deactivation, i.e., how the motion would change when the force development capacity of a muscle has been impaired, were not examined in these studies.

Human gait motion have also been simulated by combining forward dynamics and optimization [25, 1, 18, 5]. Studies have been carried out to identify the input signals to muscles that enable human gait motion in a forward dynamics environment, the objective of these studies being to obtain an accurate pattern of muscle activation during gait motion.

Although these researches have succeeded in simulating realistic normal gait, there are several shortcomings with these methods that make it difficult to apply them to analyize the effects of deactivation of individual muscles, which would involve various cases according to the patients.

First of all, the researcher must provide a good initial guess of the activation data in the beginning to avoid the optimization process to get stuck into some local minima. In most of the cases, this is done through trial-and-error by the researcher. This is quite time consuming, and the researcher needs special experience to determine the good set of muscle activations to generate realistic gait motion. Next, since all the time sequence data for the muscles must be determined through the optimization, the computational cost for these methods are enormous. Third, although balance-keeping is one of

the most important factor for gait motion, there was no explicit way to describe the balanced motion in these researches. As a result, the optimizer always had to suffer from keeping the balance while searching for the right set of parameters that generates a realistic human gait motion.

In robotics, biped locomotion of humanoid robots is one of the most exciting topics these days. Many researchers have developed humanoid robots that are capable of performing biped gait motion [10, 7, 4, 9]. A major way is to design gait motion based on Inverted Pendulum Model (IPM) [10, 9]. The IPM approach is a top down approach, comparing to the bottom approach used in biomechanics, as the abstract motion is determined first, and the details of the motion such as the kinematic data are calculated in the bottom stage. The advantage of the top down approach is that the controller does not have to suffer from detemining low level control signals such as the torque exerted at the joints or the muscle activation data in the beginning. It is possible to simplify complex models of humanoid robots that have too many degrees of freedom to be controlled directly. In addition to that, as the motion of the COG is explicitly controlled, the balance of the humanoid robot is assured in the feedforward stage. Therefore, when using optimization methods to plan motions, it is not necessary to suffer from keeping the balance.

However, no angular momentum have been generated by the IPM since it assumes that the center of gravity (COG) is a mass point and that the ground force vector always passes through the COG of the system. It is therefore difficult to generate various patterns of gait motion, particularly human-like gait motion, using this model.

In this study, we propose a new top-down approach to calculate pathological gait by combining the IPM method with the musculoskeletal model. The effects of deactivating the gluteus medialis muscles were examined and compared with real human motion data done by patients with similar disabilities.

The trajectory of the COG is first calculated by using the Enhanced Inverted Pendulum Model [11, 14] that extends the IPM by allowing angular momentum to be generated around the center of mass. Next, the kinematics of the motion is determined using inverse kinematics. As the muscles of the body that is to be deactivated is determined, an objective function based on the time series data of the force exerted by this muscle is formed. By minimizing this criteria by searching an optimal set of EIPM parameters that define the gait motion, the pathological gait motion is calculated.

The method proposed in this study has the following advantages comparing to previous methods:

- Since the gait motion is described by the EIPM parameters, there is no need to specify all the input parameters to the muscles. As a result, the computational cost for the optimization is much less than previous methods.
- As the balance of the human body model is explicitly kept by using the EIPM model, the optimizer only needs to search the optimal set of parameters in terms of muscle force, and therefore does not need to go through a large number of trials to generate the balanced motion.

2 Musculoskeltal Model

To simulate the motion by pathological patients, it is necessary to prepare a physiological model of the human body. The musculoskeletal model developed by Delp [3] was used in this study. This data includes the attachment sites of 43 muscles on each leg and physiological parameters such as the length of tendons, muscular filaments, and etc. Muscles are attached only to the legs, and no muscles are put on the upper half of the body. The human body model used in this study is shown in Figure 1.

The upper half of the body is composed of the chest, head, upper arms, lower arms, and hands. However, only the chest (3 DOF) and the upper arms (3 DOF each) are allowed to move among these segments. The lower half of the body is composed of the pelvis, and the femur, tibia, patella, talus, calcaneous, and toes in each leg. The joints of the legs are assumed as either a 3-DOF gimbal joint (hip joint) or as a 1-DOF joint (knee, ankle, calcaneous, and metatarsal joint). Therefore, the total degrees of freedom of the body, including the 6DOF of the pelvis in the global coordinate system, is 29.

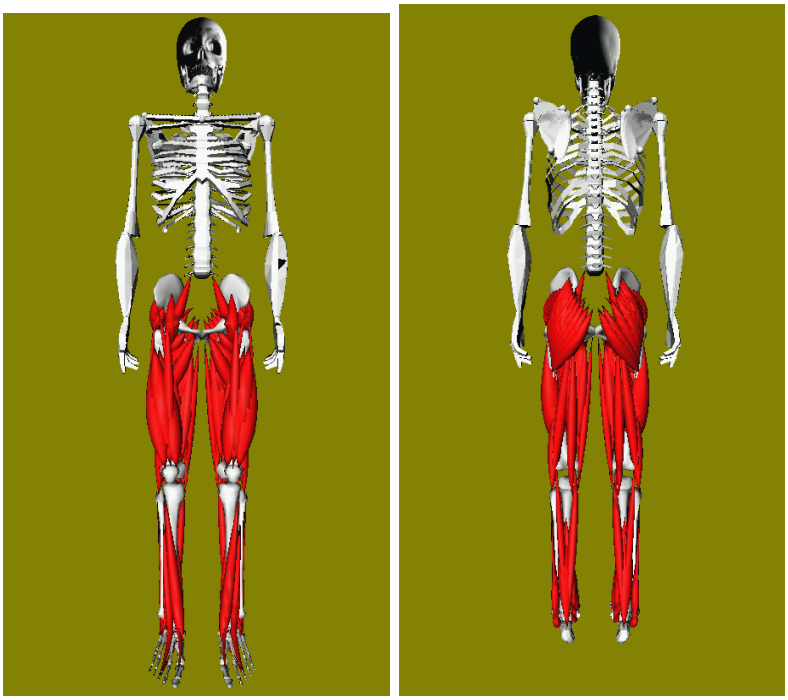

Figure 1: The frontal (left) and backward (right) views of the human body model

Each musculotendon is based on the musculotendon model of Hill [6], and parameter values were derived according to Delp [3]. The musculotendon model is composed of three elements: a contractile element (CE, representing all the muscle fibers), a parallel elastic element (PEE, representing all connective tissues around the muscles fibers), and a series elastic element (SEE, representing all series elasticity, including tendons). At each time step, the musculotendon length was determined from the posture (i.e., as a function of joint angles). Thereafter, the range of force developed by a muscle can be calculated at each time step:

$$F_m^{min} \leq F_m(t) \leq F_m^{max} \tag{1}$$

where $F_m(t)$ is the musculotendon force of the mth muscle, F_m^{min} and F_m^{max} are the minimum and maximum force developed by this muscle, which are determined by their force-length-velocity properties:

$$\begin{aligned} F_m^{min} &= f(F_m^0, l_m, v_m, 0) \\ F_m^{max} &= f(F_m^0, l_m, v_m, 1) \end{aligned}$$

where function $f(F_m^0, l_m, v_m, a_m)$ is the force-length-velocity surface assumed in the musculoskeletal model [27], l^m is the length and v^m is the velocity of the shortening muscle m, and the 0 and 1 in these equations are a_m, the activation level of the muscle that determines the amount of force exerted by the contractile element ($0 \leq a_m \leq 1$).

3 Enhanced Inverted Pendulum Model

As explained in the Introduction, the IPM is an algorithm used in robotics to plan the balanced gait motion by humanoid robots. The enhanced version of the IPM is used in this study to plan the trajectory of the COG that resembles humans.

Let us define the position of the COG by (x, H) and the position of the ZMP by $(zmp, 0)$. In the IPM, the ground force vector (F_x, F_y) had to be parallel to the vector connecting the COG and the ZMP, which is to satisfy the following law:

$$F_x : F_y = \ddot{x} : \ddot{z} + g = x : H.$$

This relationship is depicted in Figure 2(a). Although this is a quite simple and convinient model to explain the motion of the COG, the motion that could be generated was limited as no angular momentum around the COG was allowed to be made.

The enhanced version of the IPM include the following two extensions: (1) the ZMP is allowed to move over the ground, and (2) the ground force vector does not have to be parallel to the vector between the ZMP and the COG, as long as its horizontal element is linearly dependent on the COG position. As a result, rotational moment can be generated by the ground force. The relationship between the COG and the ground force with the IPM and the EIPM are depicted in Figure 2(a) and (b), respectively. Let us define here the direction of the ground force vector by $(cx + d, H)$. The

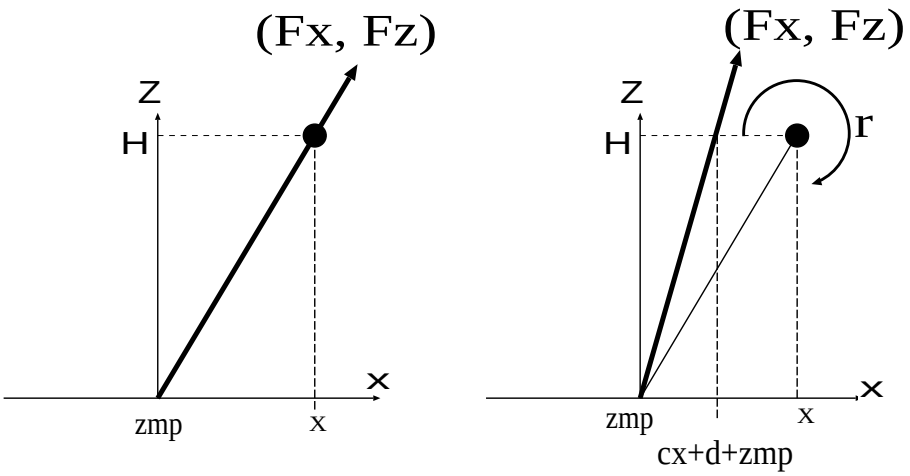

Figure 2: The standard IPM (a) and enhanced IPM (b). The IPM restricted the ground force to pass through COG while the EIPM allows the horizontal component of the ground force have linear relationship with the position of the COG.

relationship between acceleration of the motion of the COG and its position then becomes

$$F_x : F_y = \ddot{x} : \ddot{z} + g = cx + d : H.$$

Since the height of the COG is $z = H$, we can write

$$\ddot{x} = \frac{g}{H}(cx + d). \tag{2}$$

The solution for this differential equation can be written as

$$x = C_1 e^{-\frac{t}{T_e}} + C_2 e^{\frac{t}{T_e}} - \frac{d}{c}, \tag{3}$$

where $T_e = \sqrt{H/(cg)}$, and C_1 and C_2 are constant values. Since initial parameter values are set at $x = x_0$ and $\dot{x} = v_0$ at $t = 0$, the constant values C_1 and C_2 are

$$C_1 = \frac{x_0 + \frac{d}{c} - v_0 T_e}{2}, \quad C_2 = \frac{x_0 + \frac{d}{c} + v_0 T_e}{2}. \tag{4}$$

The ground force vector can then be written as

$$\begin{aligned} F_x &= m\ddot{x} = \frac{m}{{T_e}^2}\left(C_1 e^{-\frac{t}{T_e}} + C_2 e^{\frac{t}{T_e}}\right), \\ F_z &= mg \end{aligned}$$

where m is the mass of the system. The rotational moment r around the y-axis can be calculated as

$$r = -\frac{mH}{{T_e}^2}\left(C_1 e^{-\frac{t}{T_e}} + C_2 e^{\frac{t}{T_e}}\right) - mg\left(C_1 e^{-\frac{t}{T_e}} + C_2 e^{\frac{t}{T_e}} - \frac{d}{c} - zmp_x\right),$$

and angular momentum ω_{t_1,t_2} generated by the rotational momentum between time $t = t_1, t_2$ can be obtained as

$$\omega_{t_1,t_2} = m(-C_1 e^{-\frac{t_2}{T_e}} + C_2 e^{\frac{t_2}{T_e}} + C_1 e^{-\frac{t_1}{T_e}} - C_2 e^{\frac{t_1}{T_e}})(-\frac{H}{T_e} - gT_e) \tag{5}$$

$$- \quad mg(\frac{d}{c})(t_2 - t_1) + mg \int_{t_1}^{t_2} zmp_x dt + \omega_1,$$

where ω_1 is the angular momentum at $t = t_1$. Using the EIPM, it is possible to define the motion of the COG and angular momentum in the sagittal plane and the frontal plane independently. Therefore, in this study, the motion of the COG in these planes are decribed by different EIPM equations.

4 Modeling Human Gait by the EIPM

Since EIPM only allows linear relationship between the COG and the ground force vector, the gait motion must be divided into several phases to be represented by the EIPM. As the motion of the gait is assumed symmetric, the half cycle of the gait motion in the sagittal plane can be divided into four stages, by the postures known as other toe off (OTO), heel rise (HR), opposite initial contact (OIC), middle stance (MS), and toe off (TO), as shown in Figure 3. The half cycle of the motion in the frontal

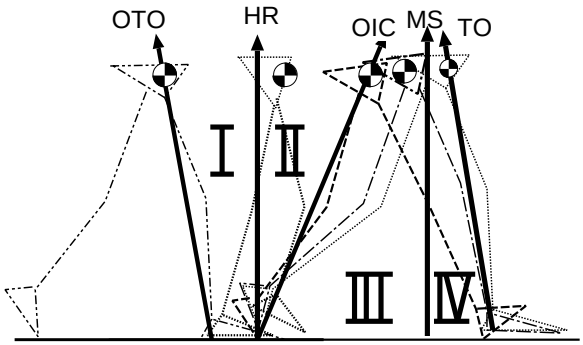

Figure 3: The half cycle of the gait is divided into four phases, each motion represented by EIPM.

plane can be represented by two consecutive EIPM models, one representing the single support phase, and the other representing the double support phase. The parameters to explain these EIPMs can be calculated from the boundary conditions and kinematic parameters of the motion. The following parameters are used to define the gait motion in this research:

- the position of COG at postures known as other toe off (OTO), heel rise (HR), and other initial contact (OIC) and its velocity at OTO in the sagital plane
- and the lateral distance between the left and right foot and the parameter that determines the angular momentum in the frontal plane.

Further explanation of these parameters can be found in Appendix A1 and A2. Let us represent these variables by vector $\boldsymbol{p}$ here.

After the trajectory of the COG and the angular momentum is determined by the EIPM, then the motion of body segments that satisfies those trajectories are calculated using inverse kinematics. It is known that methodologies of inverse kinematics combined with concepts of COG [16] and dynamics [26] give fairly realistic motions. Natural behavior such as swinging of arms and thorax can be obtained using this methodology. This process is also explained in [11] and Appendix A3. By using inverse kinematics, the values, velocities, and accelerations of the generalized coordinates can be calculated. Then, the torque developed at each joint was calculated from these kinematic data by using inverse dynamics [23]. During double support phase, to solve the redundancy problem caused by the closed-loop formed by the ground and the feet, the ground force vector was divided into two and applied to

each foot in a manner the total amount of torque exerted by the joints is minimized [17]. In summary, by specifying the variable parameters $\boldsymbol{p}$ for the EIPM, the motion of the human body model was calculated. As the kinematic data and external force data from the ground are available, the torques exerted by the joints could be calculated.

5 Calculating pathological gait

Torque $\tau_j(t)$ developed at joint j is theoretically generated as follows by the muscles crossing the joint:

$$\tau_j(t) = \sum_m F_m(t) r_{m,j}, j = 0, ..., n_{dof} \tag{6}$$

where $r_{m,j}$ is the moment arm of muscle m about the jth joint axis, and n_{dof} is the number of degrees of freedom whose torque are assumed here to be generated by the muscles. They include the flexion/extension, adduction/abduction, and rotation at the hip, flexion/extension at the knee, and plantarflexion/dorsiflexion at the ankle, and therefore, by taking into account both legs, $n_{dof} = 10$.

The muscle forces at each time step can be calculated by minimizing the muscle stress [2]:

$$J = \sum_m^{n_m} (\frac{F_m(t_i)}{F_m^0})^2 \tag{7}$$

where n_m is the total number of muscles ($n_m = 43 \times 2 = 86$), and F_m^0 is the maximal force parameter of muscle m, that is calculated by the physiological cross-sectional area of the muscle. J was minimized using quadratic programming [15], which is an optimization method that can minimize a quadratic form while satisfying linear equality and inequality constraints. In summary, the muscle forces can be calculated by minimizing Equation (7) while using Equations (6) and Equation (1) as constraints. This method is known as the static optimization method to estimate muscle force in biomechanics [1, 28].

To describe the process to calculate the pathological gait, let us define a new function here that summarize all the processes explained previously, including the EIPM, inverse kinematics, inverse dynamics and static optimization:

$$F_m = f_m(\boldsymbol{p}, t)(m = 0, ..., n_m - 1) \tag{8}$$

where $\boldsymbol{p}$ is the vector defined in section 4 that include the parameters to define the gait motin by the EIPM, and F_m is the force by muscle m calculated by minimizing Equation 7. To simulate the effect of weakening muscle m, the following criteria is minimized until it is smaller than the threshold value:

$$J_m = \int_0^T f_m(\boldsymbol{p}, t) dt + \alpha(\boldsymbol{p}, t) \tag{9}$$

where T is one cycle of the gait motion, and $\alpha(\boldsymbol{p}, t)$ is a penalty function that is based on the external torque that has to be applied to the body to assist the musculoskeletal model accomplish the motion when there is no solution found for the static optimization problem at time t [13, 12]. The penalty function helps to avoid the motion to be converged to one that is not feasible by the musculoskeletal model. This optimization is done using sequential quadratic programming [15].

6 Experimental Data Analysis

First of all, the normal gait motion was generated by setting the appropriate EIPM parameters $\boldsymbol{p}$. Next, by minimizing an objective function based on the gluteus medialis that has the form of Equation (9), the effects weakening the gluteus medialis during gait was simulated.

As the optimization proceeds, features known as lateral trunk bending appears in the motion. The trunk swings from one side to the other, producing a gait pattern known as waddling. During the

double support phase, the trunk is generally upright, but as soon as the single support phase begins, the trunk leans over the support leg, returning to the upright attitude again at the beginning of the next double support phase.

The trajectory of the gait motion before and after the optimization is shown in Figure 4 (a) and (b) as well.

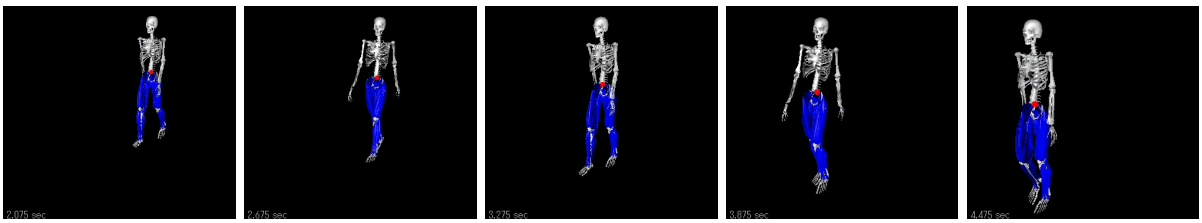

(a)

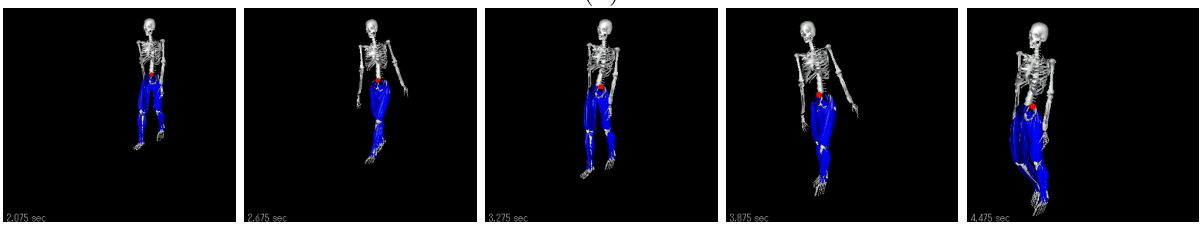

(b)

Figure 4: The trajectory of the EIPM-generated motion before (a) and after (b) the optimization..

The trajectory of the angular momentum of the body around the anterior axis before and after the optimization is shown in Figure 5 (a). Because of the waddling, a large amount of angular momentum is generated by the gait motion by the weakened gluteus medialis. The results are compared with the data by real human, that by a healthy subject and that by a patient who has congenital dislocation in Figure 5 (b). The time-series data of the muscle force calculated from the motion using the static optimization method is shown in Figure 6. The real human muscle force data estimated by the EMG pattern of muscles during normal gait from [21] are listed together. This estimation was done by multiplying the maximum force parameter F_m^0 by the activation data listed in [21], which were calculated by manual muscle tests.

7 Discussions

As we compare the muscle force calculated from the motion by the EIPM with the muscle force calculated based on the EMG data, the overall features of the time-series data are quite similar, although there are some differences such as the timing of the on-set and off-set of the muscle force, and the activation pattern of muscles such as the rectus femoris. The former gap can be due to the difference of the motion while the latter is a problem that often results from using static optimization to estimate force exerted by biarticular muscles. Similar phenomena are observed in researches such as [2, 1]. To overcome this problem, a new method to estimate muscle force by taking into account the special role of the biarticular muscles such as transferring energy from one segment to another must be proposed. This is, however, out of scope of this research. From these results we can conclude that the motion based on the EIPM is not only dynamically feasible, but also physiologically feasible.

In our experment, by minimizing the amount of force exerted by the gluteus medialis during the gait motion, the waddling gait motion was automatically induced. This is a quite natural phenomena, as it is known weak abductor muscles causes waddling. Waddling is a well-known abnormality of gait motion which is caused not only by weak abductor muscles, but also by congenital dislocation of hip joints and pain in the joints. Waddling reduces the torque and the bone-on-bone contact force at the hip of the support leg during the single support phase. As shown in Figure 6(e), the muscle force

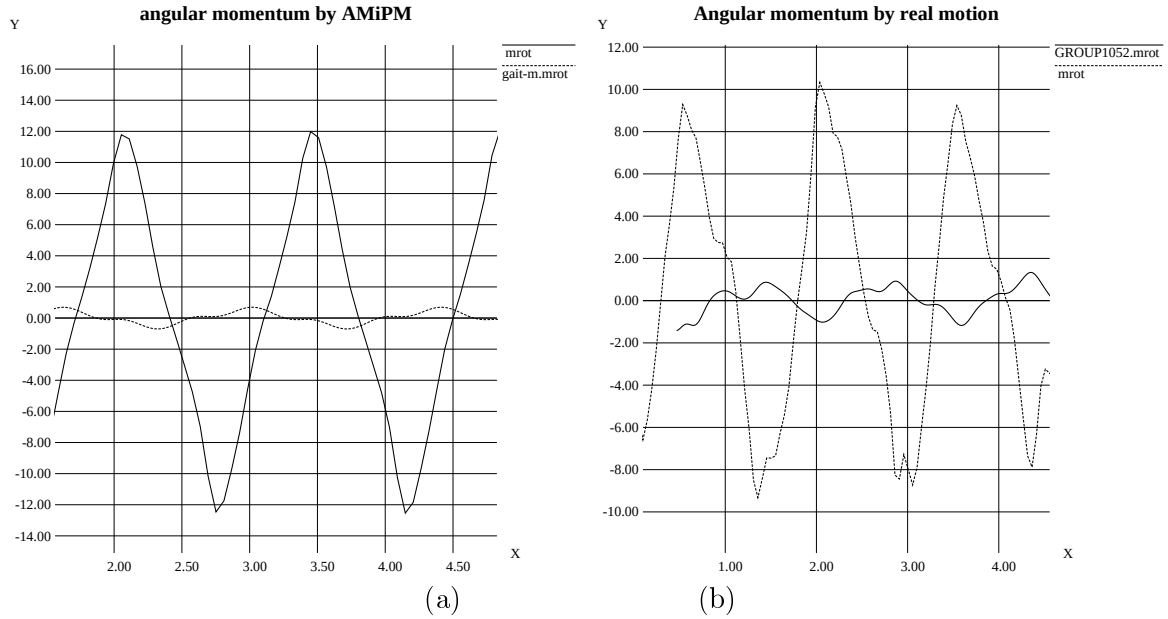

Figure 5: The comparison of the angular momentum around the anterior axis during the gait motion. (a) The data calculated by the motion created by the EIPM, before (dark line) and after (dashed line) the optimation process. The amplitude of the angular momentum increases as the force exerted by the GMED decreases. These results match with the data calculated using real human motion, which is shown in (b). In (b), the same data by a healthy subject (dark line) and a patient with waddling gait (dashed line) caused by congenital dislocation are shown.

by the gluteus medialis is greatly reduced after the optimization process. The muscle force history of real human performing normal gait and waddling gait calculated using static optimization are shown in Figure 7. The waddling gait was performed by a patient with congenital dislocation on both hip joints. The force exerted by the patient who has congenital dislocation is much less than that by the the healthy subject. In this sense, the results obtained through our experiment shows great similarities with the real human data.

As we compare the angular momentum around the frontal axis by the motion calculated using our method and by the real human data, the curves of the trajectories by normal motion and by abnormal motion both show has similarities (Figure 5).

The method used in this research to calculate human gait motion is based only on a limited number of parameters that define the motion of the EIPM. Comparing to dynamic optimization methods that have recently been used in biomechanics to simulate human gait and estimate muscle force, the method proposed in this study has the following advantages:

1. since the number of the parameters is small, the optimization converges much faster than dynamic optimization methods,

2. since the balance of the motion is assured by the algorithm of the motion generation, the optimizer does not have to suffer from keeping the balance through the gait cycle,

3. it is not necessary to search manually the initial guess of the muscle-activation parameters that decide the motion, as the parameters that define the gait based on the EIPM are intuitive kinematic parameters such as the position and velocity of the COG.

By taking into account these advantages and also the validity of the results in this study, it is possible to conclude that our method can be used as a new approach to analyze and simulate human gait under various condtions.

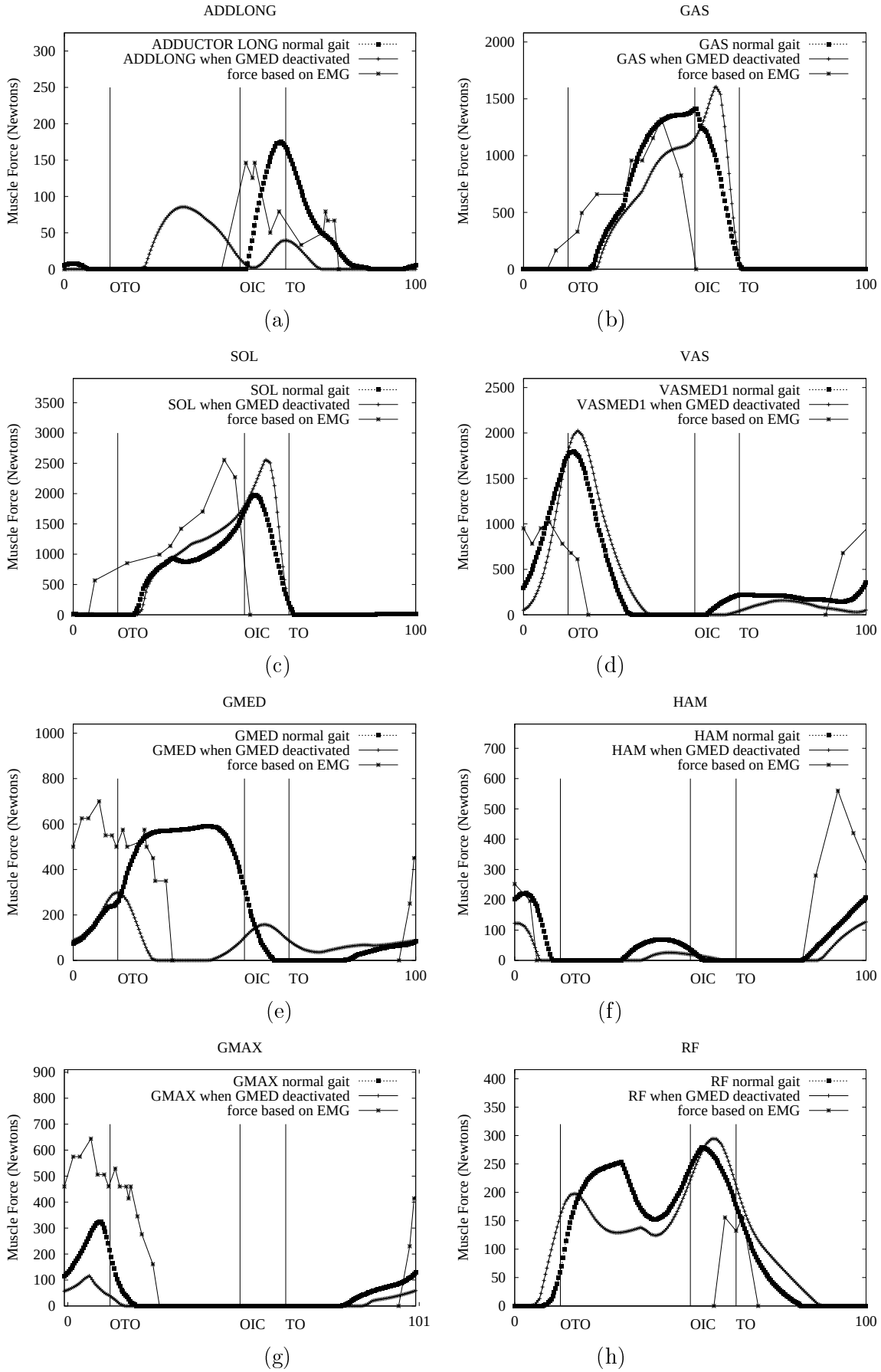

Figure 6: Muscle force characteristics of the support leg during gait (◯) and the corresponding EMG data (∗) from [21] . The figures show the characteristics of (a) adductor longus (ADDLONG) (b) gastrocnemius (GAS), (c) soleus (SOL), (d) vastus (VAS), (e) gluteus medialis (GMED), (f) hamstrings (HAM), (g) gluteus maximus (GMAX), and (h) rectus femoris (RF).

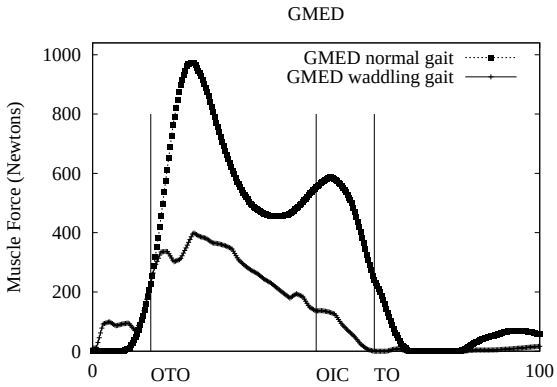

Figure 7: The GMED force calculated by static optimization method using real human motion by a healthy subject (■) and by a patient with congenital dislocation (+).

8 Summary and Future Work

In this study, we have proposed a new method to simulate the gait motion when muscles are deactivated. The method is based on the EIPM which is an enhanced model of the IPM that is often used in robotics to generate gait motion. Comparing to previous methods, the method proposed here is quite simple, and the computation cost is much less. For further research, we are planning to fit the EIPM model into real human motion data, and simulate the effects of physiological disabilities and also the process of pathology for rehabilitation use.

References

[1] Frank C. Anderson and Marcus G. Pandy. Static and dynamic optimization solutions for gait are practically equivalent. Journal of Biomechanics, 34(2):153–161, 2001.

[2] R.D. Crowninshield and Richard A. Brand. A physiologically based criterion of muscle force prediction in locomotion. Journal of Biomechanics, 14:793–800, 1981.

[3] S.L. Delp. Surgery simulation: A computer graphics system to analyze and design musculoskeletal reconstructions of the lower limb. PhD thesis, Stanford University, 1990.

[4] Yasutaka Fujimoto and Atsuo Kawamura. Robust biped walking with active interation control between robot and environment. Proceedings of IEEE AMC96, 1996.

[5] Kazunori Hase and Nobutoshi Yamazaki. Computational evolution of human bipedal walking by a neuro-musculoskeletal model. Artificial Life Robotics, 3, 1999.

[6] V Hill, A. The heat of shortening and the dynamic constants of muscle. Proc. Roy. Soc., B, 126:136–195, 1938.

[7] K Hirai, M Hirose, Y Haikawa, and T. Takenaka. The development of honda humanoid robot. Proceedings of IEEE International Conference on Robotics and Automation, pages 1321–1326, 1998.

[8] Ron Jacobs, Maarten F Bobbert, and Gerrit Jan van Ingen Schenau. Mechanical output from individual muscles during explosive leg extensions: The role of biarticular muscles. Journal of Biomechanics, 29(4):513–523, 1996.

[9] Shuuji Kajita, Osamu Matsumoto, and Muneharu Saigo. Real-time 3d walking pattern generation for a biped robot with telscopic legs. Proceedings of the 2001 IEEE International Conference on Robotics and Automation, 2001.

[10] Shuuji Kajita, Tomio Yamaura, and Akira Kobayashi. Dynamic walking control of a biped robot along a potential energy conserving orbit. IEEE Transactions on Robotics and Automation, 8(4), 1992.

[11] Taku Komura, Akinori Nagano, Shunsuke Kudoh, and Yoshihisa Shinagawa. Generating human gait using the enhanced inverted pendulum mode. Journal of Dynamics, Measurement and Control : Transactions on ASME, submitted.

[12] Taku Komura and Yoshihisa Shinagawa. Attaching physiological effects to motion-captured data. Graphics Interface Proceedings, pages 27–36, 2001.

[13] Taku Komura, Yoshihisa Shinagawa, and Tosiyasu L. Kunii. Creating and retargetting motion by the musculoskeletal human body model. The Visual Computer, (5):254–270, 2000.

[14] Shunsuke Kudoh and Taku Komura. C$\hat{2}$ continuous gait-pattern generation for biped robots. Proceedings of IEEE/RSJ International Conference on Intelligent Robots and Systems, page in press, 2003.

[15] C. T. Lawrence, J. L. Zhou, and A. L. Tits. User's guide for cfsqp version 2.5: A c code for solving (large scale) constrained nonlinear (minimax) optimization problems, generating iterates satisfying all inequality constraints. Technical Report TR-94-16r1, Institute for Systems Research, University of Maryland, 1997.

[16] R. Mas, R. Boulic, and D.Thalmann. A robust approach for the control of the center of mass with inverse kinetics. Computers and Graphics, 20(5):693–701, 199.

[17] Yoshihiko Nakamura. Advanced Robotics: Redundancy and Optimizations. Addison-Wesley, 1991.

[18] R.R. Neptune, S.A. Kautz, and F.E. Zajac. Contributions of the individual ankle plantar flexors to support, forward progression and swing initiation during walking. Journal of Biomechanics, 34:1387–1398, 2001.

[19] Benno M. Nigg and Walter Herzog. Biomechanics of the Musculo-Skeletal System, 2nd Edition. John Wiley & Son Ltd, 1999.

[20] M.G. Pandy and Felix E. Zajac. Optimal muscular coordination strategies for jumping. Journal of Biomechanics, 24:1–10, 1991.

[21] Jacquelin Perry. Gait Analysis. SLACK Incorporated, 1992.

[22] S.J. Piazza and S.L. Delp. The influence of muscles on knee flexion during the swing phase of the gait. Journal of Biomechanics, 29(6):723–33, 1996.

[23] D.A. Winter. Biomechanics and Motor Control of Human Movement. W & W. New York, NY, USA., 1990.

[24] Gary Yamaguchi. Dynamic Modeling of Musculoskeletal Motion - A Vectorized Approach for Biomechanical Analysis in Three Dimensions. Kluwer Academic Publishers, 2001.

[25] G.T. Yamaguchi and Felix E. Zajac. Restoring unassisted natural gait to paraplegics via functional neuromuscular stimulation: a computer simulation study. IEEE Transactions on biomedical engineering, 37:886–902, 1990.

[26] Katsu Yamane and Yoshihiko Nakamura. Dynamics filter - concept and implementation of on-line motion generator for human figures. Proceedings of IEEE International Conference on Robotics and Automation, pages 688–694, 2000.

[27] Felix E. Zajac. Muscle and tendon: properties, models, scaling, and application to biomechanics and motor control. CRC Critical Reviews in Biomedical Engineering, 17(4):359–411, 1989.

[28] Felix E. Zajac and Jack M. Winters. Modeling musculoskeletal movement systems: Joint and body segmental dynamics, musculoskeletal actuation, and neuromuscular control. In Jack M. Winters and Savio L-Y. Woo, editors, Multiple muscle systems: Biomechanics and movement organization, chapter 8, pages 121–147. Springer-Verlag, 1990.

Appendix

A1: Application of the enhanced IPM for calculation of motion in the sagittal plane

Since EIPM only allows linear realtionship between the COG and the ground force vector, the gait motion must be divided into several phases to be represented by the EIPM. By substituting the position and acceleration data at the boundary postures into Equation 2, the coefficients of the EIPM can be calculated for each stage. For example, as the motion of the COG is defined for the ith stage is defined by

$$\ddot{x} = \frac{g}{H}(c_i x + d_i), \tag{10}$$

where c_i and d_i are the EIPM coefficients that define the motion of the COG at this stage, they can be calculated by substituting the position and acceleration data of the COG at the beginning and end of this stage:

$$c_i = \frac{H(\ddot{x}_{i+1} - \ddot{x}_i)}{g(x_{i+1} - x_i)} \tag{11}$$

$$d_i = \frac{H(\ddot{x}x_{i+1} + \ddot{x}_{i+1}x_i)}{g(x_{i+1} - x_i)} \tag{12}$$

where x_i and $\ddot{x}_i$ are the position and acceleration of the COG in the beginning of stage i. The position of the ZMP has a linear relationship with the position of the COG:

$$zmp_x = a_i x + b_i \tag{13}$$

where a_i and b_i are constant coefficients that determine the motion of the ZMP in each stage. In the sagittal plane, the position of the ZMP at OTO, HR, OIC, and TO are set under the heel, metatarsals, and tiptoe, respectively. The position of the ZMP at MS is determined in a manner that the angular momentum around the COG at the beginning and end of half cycle are the same. The coefficients a_i, b_i can be calculated using these boundary condtions:

$$a_i = \frac{zmp_{i+1} - zmp_i}{x_{i+1} - x_i}$$

$$b_i = \frac{x_{i+1}zmp_i - x_i zmp_{i+1}}{x_{i+1} - x_i}$$

where zmp_i is the position of the zmp on the beginning of stage i. Among the variables described above, the following parameters are used for the optimization:

- the position of COG at OTO, HR, OIC, and
- the velocity at OTO.

The position of the COG at MS is determined in a manner to compensate the angular momentum generated during the single support phase. Therefore, the number of parameters for the EIPM in the sagital plane is 4.

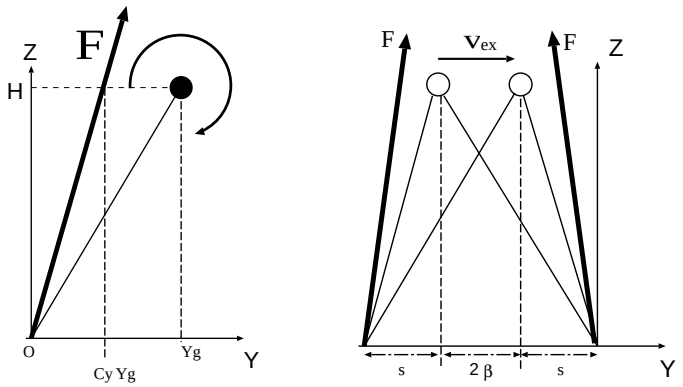

(a) (b)

Figure 8: Coordinate systems used in the frontal plane for (a) the single support phase and (b) the double support phase. The origin is set to the position of the ZMP in the single support phase and to the center in the double support phase.

A2: Application of the enhanced IPM for calculation of motion in the frontal plane

The coordinate systems used here are shown in Figure 8. The distance between the feet when they are both on the ground is $2s + 2\beta$. The COG moves 2β during the double support phase. After switching to the single support phase, it moves along until it stops and returns back the same path. The relationships between the ZMP, COG and ground force during the single support phase are

$$\ddot{y_g} : \ddot{z_g} + g = c_y y_g : H, \tag{14}$$

where c_y is a constant value that is correlated with ground force direction and position of the COG (Figure 8(b)). Using the terminal condition, the motion of the COG can be finally written as:

$$y_g = s \cosh \frac{t}{T_{ls}} - v_{ex} \sinh \frac{t}{T_{ls}}, \tag{15}$$

where v_{ex} is the velocity when the single support starts, and $T_{ls} = \sqrt{H/(c_y g)}$. Since the duration of the single support phase T is determined by the motion in the sagittal plane ($T = t_2 - t_0$), v_{ex} can be calculated by setting $t = T, y_g = s$ in Equation 15. As a result, v_{ex} can be calculated as

$$v_{ex} = \frac{-s + s \cosh \frac{T}{T_{ls}}}{\sinh \frac{T}{T_{ls}}}.$$

The y-component of the ground force can be written as

$$\begin{aligned} F_y &= \frac{m}{T_{ls}^2} \left(y_0 \cosh \frac{t}{T_{ls}} - v_{ex} \sinh \frac{t}{T_{ls}} \right), \\ F_z &= -mg. \end{aligned}$$

Since the trajectories of the ground force, COG, and ZMP are known, rotational moment around the anterior axis can be calculated as

$$r_x = y_g F_z - H F_y.$$

The double support phase can be modeled as follows. Since the motion in the frontal plane is symmetric with respect to time, it can be considered that the ZMP and COG satisfy the following relationship:

$$z_y = \frac{\beta}{\beta + s} y_g.$$

Since rotational momentum is generated in the frontal plane and since rotational momentum decreases as the COG approaches the origin of the coordinate system, motion of the COG can be approximated by the following function:

$$\ddot{y_g} : g = c_3(y_g - z_y) : H, \tag{16}$$

where c_3 is a constant. Using the boundary conditions of the single support phase, c_3 can be calculated as

$$c_3 = \frac{\beta + (1 - a_{cogy})s}{\beta} < 0.$$

The trajectory of y_g then becomes

$$y_g = C_1 \cos \frac{t - t_2}{T_c} + C_2 \sin \frac{t - t_2}{T_c} - \frac{b}{T_c^2},$$

where C_1 and C_2 are arbitrary constant values. Using the terminal conditions, the final form becomes

$$y_g = (\beta + s) \cos \frac{t - t_2}{T_c} + v_e x \sin \frac{t - t_2}{T_c}.$$

The y and z components of the ground force can be written as

$$\begin{aligned} F_y &= -\frac{m}{T_c^2}\left((\beta + s) \cos \frac{t - t_2}{T_c} + v_{ex} \sin \frac{t - t_2}{T_c}\right), \\ F_z &= -mg. \end{aligned}$$

Rotational moment around the anterior axis can be calculated by using Equation 16. As same as in the sagittal plane, because of the symmetry of the motion with respect to time, we do not have to tune any parameters to compensate for the angular momentum. The variables used for optimization in the frontal plane are only c_y and s.

A3: Calculating the joint angles using inverse kinematics

As we have already defined trajectories of the COG and angular momentum, the next step is to calculate kinematic parameters that satisfy these trajectories. Invese kinematics is used for this purpose. At first, positions and rotational trajectories of the feet, which are defined here as (p_l, θ_l) and (p_r, θ_r), are calculated using footstep data specified in advance. As shown in Figure 9, four keyframes of the support foot are specified. The data include posture of the foot at initial contact, initial full contact, heel rise, and toe-off. The x- component of the velocity of the motion of the foot

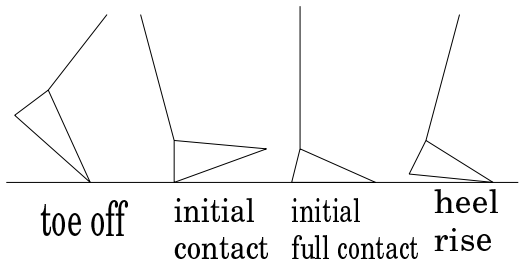

Figure 9: Keyframes of the foot rotation

of the swing leg when it is lifted from the ground is calculated by

$$v^0_{swing} = \frac{l_s}{T_{swing}}.$$

The final velocity of the motion of the foot when it comes into contact with on the ground is set to zero. The trajectory of the swung foot is calculated by intepolating the keyframes with a cubic spline curve.

Trajectories of generalized coordinates of the human body model are defined here as $\boldsymbol{q(t)} = (q_1(t), q_2(t), ..., q_{dof}(t))$, where dof is the number of degrees of freedom of the human body model, which is actually twenty nine as explained in Section 2.

The relationship between velocity of the motion of the COG and velocity of the motion of the generalized coordinates can be written as follows:

$$\dot{\boldsymbol{x_g}} = \boldsymbol{J_{cog}}\dot{\boldsymbol{q}},$$

where J_{cog} is the Jacobian matrix that consists of the partial differentials of the COG by the generalized coordinates:

$$\boldsymbol{J_{cog}} = \frac{\partial \boldsymbol{x_g}}{\partial \boldsymbol{q}}.$$

Acceleration of the motion of the COG can then be obtained as follows:

$$\ddot{\boldsymbol{x_g}} = \boldsymbol{J_{cog}}\ddot{\boldsymbol{q}} + \dot{\boldsymbol{J}}_{\boldsymbol{cog}}\dot{\boldsymbol{q}}. \tag{17}$$

Angular momentum r and the first derivative of the generalized coordinates have a linear correlation:

$$\boldsymbol{r} = \boldsymbol{R}\dot{\boldsymbol{q}}.$$

The derivative of the angular momentum can then be calculated as follows:

$$\dot{\boldsymbol{r}} = \boldsymbol{R}\ddot{\boldsymbol{q}} + \dot{\boldsymbol{R}}\dot{\boldsymbol{q}}. \tag{18}$$

Acceleration of the motions of the feet can be expressed as functions of $\ddot{\boldsymbol{q}}$

$$\begin{pmatrix} \ddot{\boldsymbol{p}}_l \\ \ddot{\boldsymbol{p}}_r \\ \ddot{\boldsymbol{\theta}}_l \\ \ddot{\boldsymbol{\theta}}_r \end{pmatrix} = \boldsymbol{J_f}\ddot{\boldsymbol{q}} + \dot{\boldsymbol{J}}_{\boldsymbol{f}}\dot{\boldsymbol{q}}. \tag{19}$$

By combining Equations 17, 18 and 19, linear constraints that must be satisfied can be written in the following form:

$$\dot{\boldsymbol{\lambda}} = \boldsymbol{J_{all}}\ddot{\boldsymbol{q}} + \dot{\boldsymbol{J}}_{\boldsymbol{all}}\dot{\boldsymbol{q}}, \tag{20}$$

where $\boldsymbol{\lambda} = (\dot{\boldsymbol{x}}_{\boldsymbol{g}}, \boldsymbol{r}, \dot{\boldsymbol{p}}_{\boldsymbol{l}}, \dot{\boldsymbol{\theta}}_{\boldsymbol{l}}, \dot{\boldsymbol{p}}_{\boldsymbol{r}}, \dot{\boldsymbol{\theta}}_{\boldsymbol{r}})^{\boldsymbol{T}}$, and $\boldsymbol{J_{all}} = (\boldsymbol{J_{cog}}, \boldsymbol{R}, \boldsymbol{J_f})^{\boldsymbol{T}}$. Calculating $\ddot{\boldsymbol{q}}$ that satisfies Equation 22 can be considered as an inverse kinematics problem.

Since this is a problem to calculate a stable gait motion, $\ddot{q}$ that minimizes the following quadratic form is calculated as

$$(\ddot{\hat{\boldsymbol{q}}} - \boldsymbol{k}(\hat{\boldsymbol{q}} - \hat{\boldsymbol{q}}_{\boldsymbol{0}}) + \boldsymbol{d}\dot{\hat{\boldsymbol{q}}})(\ddot{\hat{\boldsymbol{q}}} - \boldsymbol{k}(\hat{\boldsymbol{q}} - \hat{\boldsymbol{q}}_{\boldsymbol{0}}) + \boldsymbol{d}\dot{\hat{\boldsymbol{q}}})^{\boldsymbol{T}}, \tag{21}$$

where $\ddot{\hat{\boldsymbol{q}}}$ is the subset of $\ddot{q}$ that determines upright posture of the body. Those parameters include rotation of the pelvis and joint angles of the chest. $\hat{\boldsymbol{q}}_{\boldsymbol{0}}$ is the target posture to keep the body upright, which is a zero vector here, $\boldsymbol{k}$ is the vector of elastic constants, and $\boldsymbol{d}$ is the vector of viscosity constants. $\ddot{\boldsymbol{q}}$ that minimizes Equation 21 and satisfies Equation 22 was calculated by quadratic programming.

The initial posture at OTO that satisfies the COG and feet position constraints is first calculated by adjusting the position of the pelvis. The velocity at the initial posture is calculated by solving for the initial generalized velocity $\dot{q}_0$ that satisfies the constraints of the COG, angular momentum, and feet:

$$\boldsymbol{\lambda_0} = \boldsymbol{J^0_{all}}\dot{\boldsymbol{q}}_{\boldsymbol{0}} \tag{22}$$

where λ_0 is the initial velocity vector and $\boldsymbol{J^0_{all}}$ is the initial Jacobian matrix for the whole system. Using the calculated acceleration, the values of the generalized coordinates and their velocites were updated step by step, and, finally, the entire trajectories were obtained.